

Low Energy Neutrinos in Super-Kamiokande: Past Successes, New Results, and Future Plans

M.B. Smy for the Super-Kamiokande Collaboration

Presenter: M.B. Smy (msmy@uci.edu), usa-smy-M-abs1-he22-oral

Electrons in the Super-Kamiokande detector have been analyzed between a total energy of 4.5 and 100 MeV for Super-Kamiokande-I and between 7 and 20 MeV for Super-Kamiokande-II. Final results for Super-Kamiokande-I as well as preliminary results for Super-Kamiokande-II are presented and perspectives for Super-Kamiokande-III discussed.

1. Introduction

Super-Kamiokande (SK) is a 50,000 metric ton water Cherenkov detector further described in [1]. Using the emitted Cherenkov light in water, electrons are detected and their vertex, direction and energy are reconstructed. In SK-I (1496 live days between May 31st, 1996 and July 15th, 2000; $\approx 40\%$ of the detector surface is covered by 20" photomultiplier tubes) electrons above a threshold total energy of 4.5 MeV are analyzed. In SK-II (so far 622 live days between December 10th, 2002 and March 19th, 2005; $\approx 20\%$ of the detector surface is covered), the analysis threshold is at present 7.0 MeV. SK-III will start about July 2006 ($\approx 40\%$ coverage).

2. Solar Neutrinos

SK detects recoiling electrons from elastic scattering of high energy ${}^8\text{B}$ (and *hep*) solar neutrinos. The cross section is strongly forward-peaked, so the directional distribution (with respect to the solar direction) shown in Figure 1 serves both as evidence that solar neutrinos originate from the sun and as a method to statistically separate solar neutrinos (shaded region) from background (dotted region) which is almost isotropic. Assuming a pure e flavor composition and the expected spectrum, SK-I measures the solar ${}^8\text{B}$ neutrino flux to be $2.35 \pm 0.02(\text{stat}) \pm 0.08(\text{syst}) \times 10^6/\text{cm}^2\text{s}$, and SK-II sees $2.36 \pm 0.06(\text{stat})^{+0.16}_{-0.15}(\text{syst}) \times 10^6/\text{cm}^2\text{s}$ (preliminary). At low energy (< 7 MeV) the background shown in Figure 1 is mostly coming from radioactive decays from the glass of the photomultiplier tubes. Above 8 MeV, the background is due to cosmic ray μ spallation. Statistically subtracting this background, positrons above a total energy of 8 MeV in the angular region below $\cos\theta_{\text{Sun}} < 0.5$

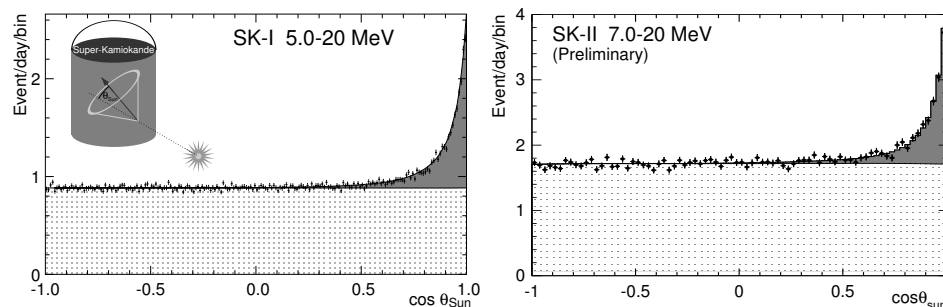


Figure 1. Angular Distribution of Solar Neutrino Event Candidates in SK-I (Left) and SK-II (Right).

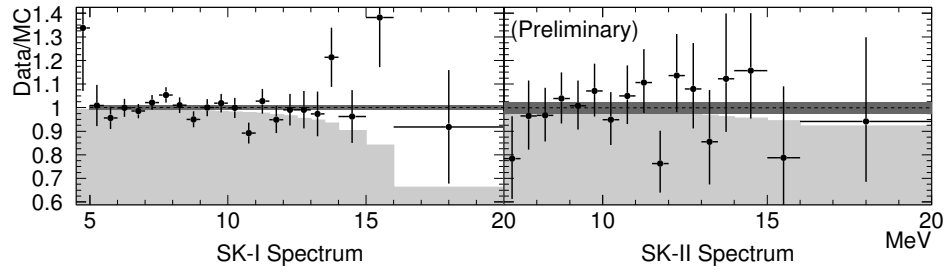


Figure 2. Recoil Electron Spectra.

limit the solar anti-neutrino flux (interacting via inverse β decay, the angular distribution of which is almost flat) to be less than $4 \cdot 10^4/\text{cm}^2\text{s}$ (90% C.L.) [2] assuming a ${}^8\text{B}$ anti-neutrino spectrum. Below 8 MeV, a limit can be obtained from a slight backward bias of the inverse β cross section: the ${}^8\text{B}$ anti-neutrino flux is $< 2 \cdot 10^6/\text{cm}^2\text{s}$ (5–6 MeV) and $< 4 \cdot 10^5/\text{cm}^2\text{s}$ (6–7 MeV, 7–8 MeV) at 90% C.L..

2.1 Solar Neutrino Oscillations

Neutrinos undergo flavor oscillations [3], therefore solar neutrinos can change their flavor from pure e during the flight to Earth (vacuum oscillations) or resonantly convert in the sun due to the high solar matter density (MSW oscillations [4]). The conversion depends on neutrino mixing $\sin^2 \theta$ and difference in mass² Δm^2 . All (active) flavors undergo neutrino–electron elastic scattering, however, the cross section for ν_e is about six times higher than the other flavors, and the observed interaction rate changes when the flavor composition changes. The flavor change due to neutrino oscillations depends on the neutrino energy, thereby distorting the observed recoil energy spectrum. Figure 2 (the dark band is the event rate between 5 and 20 MeV for SK-I and 7–20 MeV for SK-II) shows the observed spectrum divided by the expected spectrum based on the pure ν_e fluxes $2.36 \cdot 10^6/\text{cm}^2\text{s}$ (${}^8\text{B}$) and $15 \cdot 10^3/\text{cm}^2\text{s}$ (*hep*). The light shaded region shows the contribution of ${}^8\text{B}$ MC alone. We do not find evidence for the presence of *hep* neutrinos: Between 18.0 and 21.0 MeV, we find 4.9 ± 2.7 solar neutrino events which limits the *hep* neutrino flux to be below $73 \cdot 10^3/\text{cm}^2\text{s}$ at 90% C.L. (assuming no oscillation). Matter effects inside the Earth on neutrino oscillations may also induce a dependence of the observed interaction rate on the solar zenith angle. The “day/night asymmetry” $A=(D-N)/(0.5(D+N))$ measures the amplitude of this variation. An amplitude fit [5] to SK-I data corresponds to an asymmetry of $-1.7\% \pm 1.6\%(\text{stat})_{-1.2}^{+1.3}(\text{syst}) \pm 0.04\%(\Delta m^2)$ where the last uncertainty is due to the uncertainty in Δm^2 . For SK-II data we split the data sample into “day” and “night” between 7.5 and 20 MeV and directly calculate the day/night asymmetry to $+1.4\% \pm 4.9\%(\text{stat})_{-2.5}^{+2.4}(\text{syst})$ (preliminary). In summary, we observe no significant spectral distortion or zenith angle dependence. SK-I data [5, 6] excludes the vacuum oscillation region near $\Delta m^2 \approx 10^{-5} (\text{meV})^2$ and the small mixing angle region $\sin^2 \theta < 0.01$ through absence of spectral distortion, as well as the MSW low Δm^2 region near maximal mixing $\sin^2 \theta \approx 0.5$ and $\Delta m^2 \approx 0.1 (\text{meV})^2$ (inconsistent solar zenith angle variation). The remaining MSW large mixing angle (LMA) region near $\sin^2 \theta \approx 1/3$ and $\Delta m^2 \approx 10 - 100 (\text{meV})^2$ is constrained to the higher $\Delta m^2 > 30 (\text{meV})^2$ (absence of significant solar zenith angle variation). The SK-I day/night asymmetry favors the Δm^2 range of $50\text{--}120 (\text{meV})^2$ at the 1σ level.

The Homestake experiment [7] detects charged-current solar neutrino interactions on Cl with an energy threshold of 0.85MeV. It therefore measures only ν_e 's. The observed SK interaction exceeds the prediction based on the Homestake rate, unless there are other, active flavors than e present in the solar neutrino flux (or the solar neutrino spectrum is distorted). Since only active neutrino flavors explain the excess, pure sterile oscil-

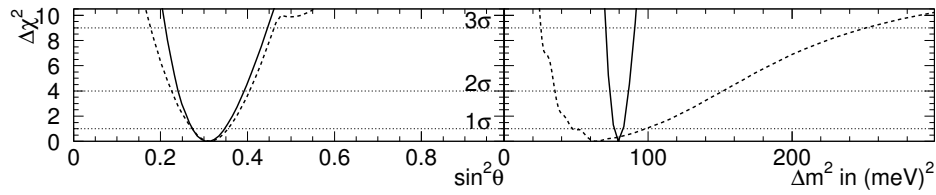


Figure 3. $\Delta\chi^2$ Versus Oscillation Parameters.

lations are excluded [6]. The SNO experiment finds the charged-current interaction rate of solar neutrinos on deuterium above $E_\nu > 8.2$ MeV to be consistent with the Homestake rate and interpretes the SK rate excess (over a prediction based on the SNO rate) as evidence for active flavor conversion. The energy threshold of SNO is somewhat higher than SK, but closer to SK's than Homestake's. The dashed lines of Figure 3 shows the χ^2 difference of a combined fit to SK and the SNO salt-phase results [9]. The fit represented by the solid lines include the KamLAND reactor anti-neutrino rate and spectrum [10] which independently confirms the solar neutrino oscillation region. The best-fit parameters are $\sin^2\theta = 0.31$ and $\Delta m^2 = 79$ (meV) 2 . For those parameters, the total ^8B flux fits best to $4.98 \cdot 10^6/\text{cm}^2\text{s}$ and the hep flux to $31 \cdot 10^3/\text{cm}^2\text{s}$. The spectra shown in Figure 2 use the ratio of these two fitted fluxes for the MC prediction. The fit constrains only the well-known reactor anti-neutrino flux, not the solar neutrino fluxes. If we confine Δm^2 to the 3σ range 70–90 (meV) 2 allowed by the fit, the expected SK-I day/night asymmetry ranges from -1.7% to -1.0% while $-1.7\% \pm 1.6\%(\text{stat}) \pm 1.3\%(\text{syst}) \pm 0.04\%(\Delta m^2)$ is observed. If the neutrino has a magnetic moment, the electromagnetic contribution to elastic scattering decreases more strongly with energy than the weak contribution. The SK-I recoil electron spectrum shape (consistent with only the weak contribution) limits the magnetic moment of the neutrino to be below $1.1 \cdot 10^{-10} \mu_B$ [11] (taking into account the neutrino oscillation distortions).

2.2 Supernova Relic Neutrinos

Core-collapse supernovae produce very large numbers of neutrinos of all flavors; they should have occurred everywhere and at all times since stars first formed. SK is mostly sensitive to anti-neutrinos of flavor e which interact with protons via inverse β decay. Due to the large distance, individual supernovae cannot be detected (except for those occurring in our own galaxy) and the positrons from the supernova relic neutrinos are uniform in direction and time. Cosmic μ spallation products is the dominant background to this measurement: Since only a few events per year are expected, remaining spallation background limits the search to $E_\nu > 19.3$ MeV. In that energy window, the remaining backgrounds are Michel electrons from (near-)invisible μ 's (no Cherenkov light was detected from the μ , since it was below or close to Cherenkov threshold) and atmospheric ν_e . No excess over these backgrounds are observed, the data limit the supernova relic neutrino flux in that energy range to be below $1.2/\text{cm}^2\text{s}$ at 90% C.L. [12]. Theoretical calculations range from 0.14–0.46 $f_*/\text{cm}^2\text{s}$ [13] where the correction factor f_* depends on the cosmic star formation rate (in the range 1–2.3).

3. Future Low Energy Measurements at Super-Kamiokande

While $\approx 1/3$ of the high energy solar neutrinos remain ν_e 's, more than half of the low energy solar neutrinos (inferred from the charged-current solar neutrino interaction rates on Gallium [14] which has a threshold of 0.24 MeV) don't change flavors. For LMA, low energy solar neutrinos oscillate with the averaged vacuum probability $2 \sin^2\theta(1 - \sin^2\theta)$ and high energy solar neutrinos with the MSW probability $(1 - \sin^2\theta)$. SK-III plans to explore the transition region between both cases by achieving a lower energy threshold than SK-I.

Between 4 and 4.5 MeV of total recoil electron energy, LMA predicts a rate enhancement of 10% over the expectation from an undistorted spectrum. SK-III hopes to achieve a lower threshold since the Radon emitted by the photomultiplier tubes is contained by the acrylic/fiberglass enclosures which prevent implosion chain reactions. Also, improvements in event reconstruction yields a better discrimination between background produced by the photomultiplier tubes (concentrated near the detector edge) and neutrino interactions (uniformly distributed): We demonstrated successful reconstruction of 4.9 MeV electrons in SK-II (which emit as much light as 2.7 MeV electrons in SK-III) injected by a linear accelerator. Using Monte Carlo simulations, we expect to be able to reconstruct 3 MeV electrons in SK-III. Studying the recoil electron spectrum below 5 MeV will also improve the sensitivity to magnetic moment interactions of solar neutrinos.

The ability to detect neutrons in SK is valuable, since it allows to tag anti-neutrinos which interact via inverse β decay. Neutrons are usually captured on hydrogen $\approx 100\mu\text{s}$ after the interaction and a single 2.2 MeV γ is emitted. Detection of these γ 's is rather difficult, since the scattered Compton electrons are below or near Cherenkov threshold. A new idea is the addition of 0.1% GdCl_3 salt to SK [15]. The Gd nuclei capture neutrons after $\approx 30\mu\text{s}$ with a much higher cross section than the hydrogen captures and emit several γ 's of a total energy of 8 MeV. The varying γ multiplicity generates an effective Gd neutron capture spectrum peaking at about 5 MeV. With an energy threshold of 3 MeV, more than 90% of the neutrons can be detected. Background events will probably prevent lowering the analysis threshold for single recoil electrons from neutrino interactions below 4 MeV. However, for an anti-neutrino interaction we can exploit the temporal and spatial correlation of positron emission and neutron capture and eliminate the background while still keeping about 80% of the anti-neutrinos. Demanding a spatial coincidence also eliminates mis-reconstructed events and ensures a good, reliable measurement of the positron energy. Due to its large target mass, a GdCl_3 enhanced SK could measure the reactor anti-neutrino spectrum with high accuracy and measure the solar neutrino oscillation parameters at the % level. Detecting neutron captures will also overcome the cosmic μ spallation background to supernova relic anti-neutrino interactions and allow a much wider energy range for this analysis (about 10-80 MeV). The other important background (decay electrons from near-threshold μ 's) is also reduced.

References

- [1] S.Fukuda et al., Nucl. Instrum. Methods A 501, 418 (2003).
- [2] Y.Gando et al., Phys. Rev. Lett. 90, 171302 (2003).
- [3] Y.Fukuda et al., Phys. Rev. Lett. 81, 1562 (1998).
- [4] S.P.Mikheyev and A.Y.Smirnov, Sov. Jour. Nucl. Phys. 42, 913 (1985); L.Wolfenstein, Phys. Rev. D 17, 2369 (1978).
- [5] M.B.Smy et al., Phys. Rev. D 69, 011104 (2004).
- [6] S.Fukuda et al., Phys. Rev. Lett. 86, 5656 (2001).
- [7] B.T.Cleveland et al., Astrophys. J. 496, 505 (1998).
- [8] Q.R.Ahmad et al., Phys. Rev. Lett. 87, 71301 (2001).
- [9] B.Aharmim et al., *nucl-ex/0502021* (2005).
- [10] T.Araki et al., Phys. Rev. Lett. 94, 081801 (2004).
- [11] D.W.Liu et al., Phys. Rev. Lett. 93, 021802 (2004).
- [12] M.Malek et al., Phys. Rev. Lett. 90, 061101 (2002).
- [13] S.Ando and K.Sato, New J. Phys. 6, 170 (2004.)
- [14] V.Gavrin, Nucl. Phys. B (Proc. Suppl.) 118, 39 (2003); T.Kirsten, Nucl. Phys. B (Proc. Suppl.) 118, 33 (2003).
- [15] J.F.Beacom and M.R.Vagins, Phys. Rev. Lett. 93, 171101 (2004.)